Electronic Supplementary Information

Inhibition of thioredoxin reductase and upregulation of apoptosis genes for effective anti-tumor sono-chemotherapy by meso-organosilica nanomedicines

Mengwen Li[ab], Yue Tian[a], Xiaoming Wen[ab], Jingke Fu*[c], Jianyong Gao*[d], Yingchun Zhu*[a]
[a]Key Laboratory of Inorganic Coating Materials CAS, Shanghai Institute of Ceramics, Chinese Academy of Sciences, Shanghai 200050, China
[b]Center of Materials Science and Optoelectronics Engineer, University of Chinese Academy of Sciences, Beijing 100049, China
[c]Shanghai Key Laboratory of Orthopaedic Implant, Department of Orthopaedic Surgery, Shanghai Ninth People's Hospital, Shanghai Jiao Tong University School of Medicine; Shanghai Engineering Research Center of Innovative Orthopaedic Instruments and Personalized Medicine, Shanghai 200011, PR China.
[d] Department of Stomatology, Changhai Hospital, Second Military Medical University, 168 Changhai Road, Shanghai 200433, China
E-mail: yongjiangao1976@126.com; yzhu@mail.sic.ac.cn

Contents

1. Supplementary methods

1.1 Enzyme-linked immuno-sorbent assay (ELISA)

The expression of p62 and LC3 II in 4T1 tumor cells after various treatments was measured using ELISA (Enzyme Linked Immunosorbent Assay) kits purchased from Enzo Life Sciences and Cell Biolabs, Inc., respectively. All tests were performed in triplicate according to the manufacturer's instructions.

1.2 In vivo pharmacokinetic assay

The pharmacokinetics of CQ@MOS was determined by measuring the Si element content at various time points. Initially, CQ@MOS in saline (30 mg/kg) was intravenously injected into female ICR mice (n=3). Subsequently, 50 μL of blood was collected at indicated time points (0, 0.25, 0.5, 1, 4, 8, 12 and 24 h). The Si content in each blood sample was then quantitatively determined by ICP-MS, and the in vivo blood circulating half-life was calculated by a double-compartment pharmacokinetic model.

The excretion of CQ@MOS was investigated by detecting the Si element levels in feces and urine at indicated time points. First, female ICR mice were divided into four groups (n=3) and CQ@MOS (30 mg/kg) was then intravenously injected into the mice. At 6, 12, 24 and 48 h of post-injection, feces and urine of mice were collected, and the Si content in them were determined by ICP-MS.

The in vivo biodistribution of CQ@MOS in various organs and tumors was evaluated. Initially, female tumor-bearing BALB/c nude mice were divided into four groups (n=3) with a tumor volume of 100 mm^3. Subsequently, CQ@MOS in saline (30 mg/kg) was injected intravenously into the mice. At 6, 12, 24 and 48 h of post-injection, the mice were euthanized, and their major organs and tumors were dissected, washed, weighted and homogenized. The Si content in the organs and tumors was quantified by ICP-MS.

2. Supplementary figures

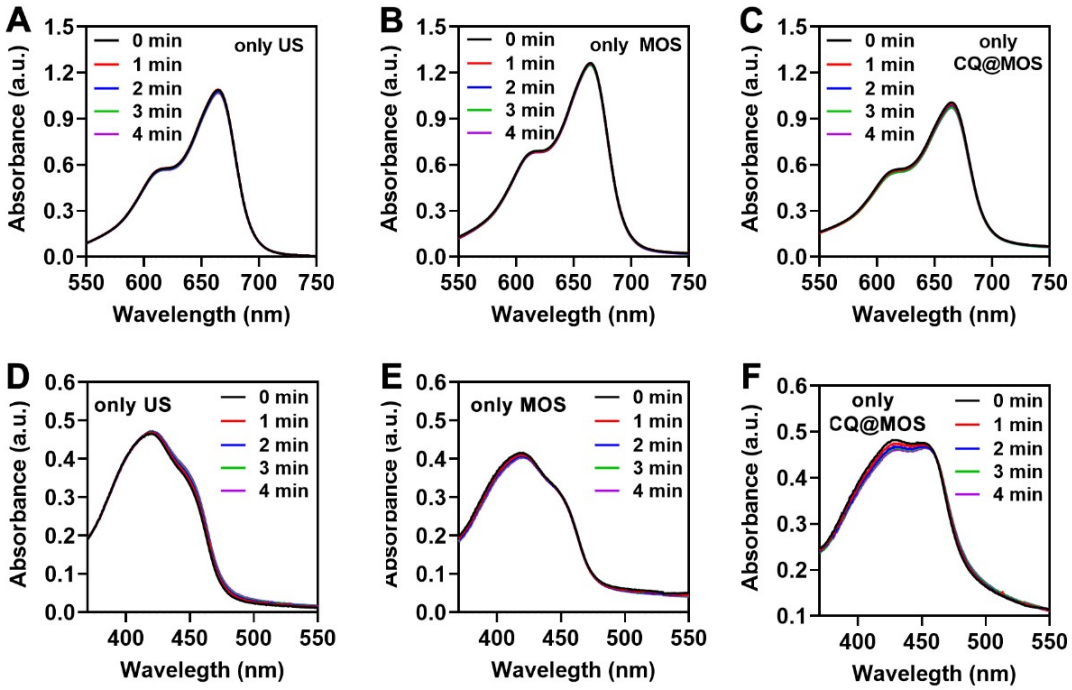

Figure. S1| Time-dependent oxidation of MB and DPBF under ultrasound (US) alone, MOS alone and CQ@MOS alone.

US, MOS and CQ@MOS alone cannot lead to the degradation of MB and DPBF, indicating the absence of reactive oxygen species (ROS) production.

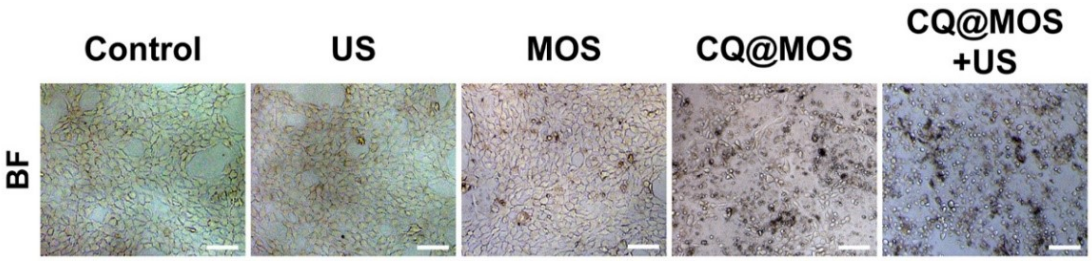

Figure. S2| Bright field pictures of Calcein/PI staining of 4T1 cells after various treatments for 24 h. Scale bar: 100 μm.

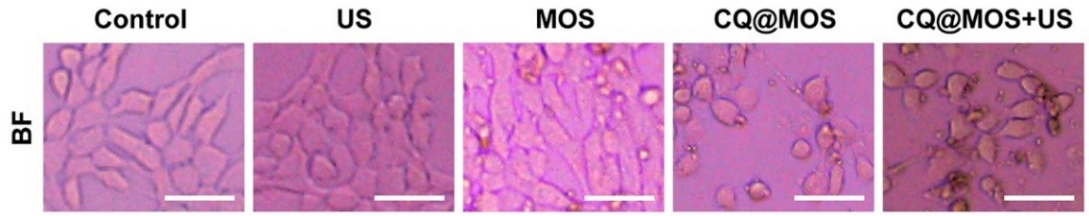

Figure. S3| Bright field images of ROS staining of 4T1 cells after various treatments for 4 h. Scale bar: 50 μm.

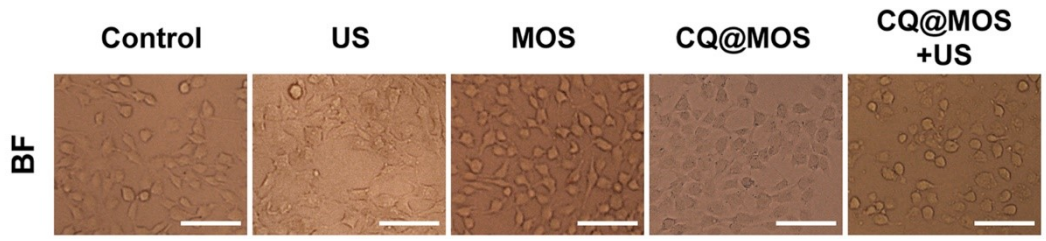

Figure. S4| Bright field images of mitochondrial membrane potential of 4T1 cells following different treatments, as determined using the JC-1 probe. Scale bar: 50 μm.

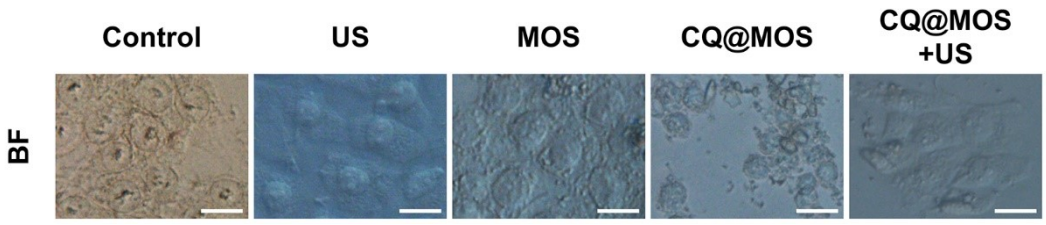

Figure. S5| Bright field images of 4T1 cells following specified treatments with DAPI as the apoptosis indicator. Scale bar: 20 μm.

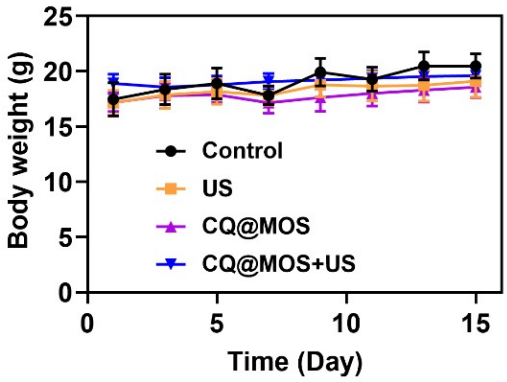

Figure S6| Body weight of 4T1 tumor-bearing nude mice over the 15-day treatment period in different groups via intra-tumoral injection (n=5 biologically independent samples).

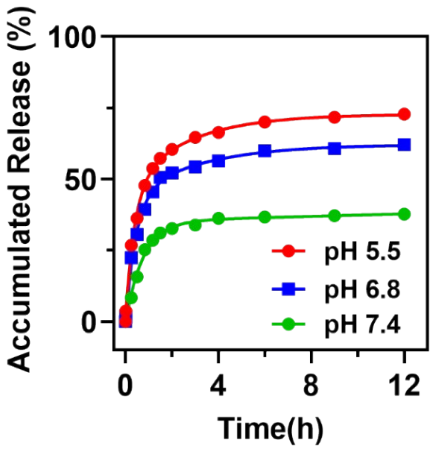

Figure S7| The release curves of CQ from CQ@MOS under various pH.

The drug release of CQ@MOS increases with the decrease of pH value from pH 7.4 to pH 6.8 and pH 5.5. This difference is attributed to the increased of the protonation of CQ under low pH conditions.

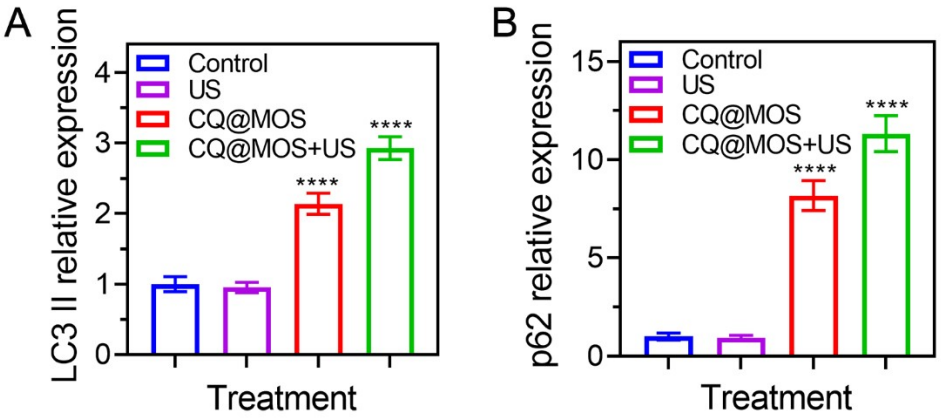

Figure S8| The expression of LC3 II (A) and p62 (B) in 4T1 tumor cells after various treatments (n=3).

Under CQ@MOS and CQ@MOS+US treatments, the expression of LC3 II and p62 in 4T1 tumor cells were significantly upregulated compared to the control groups.

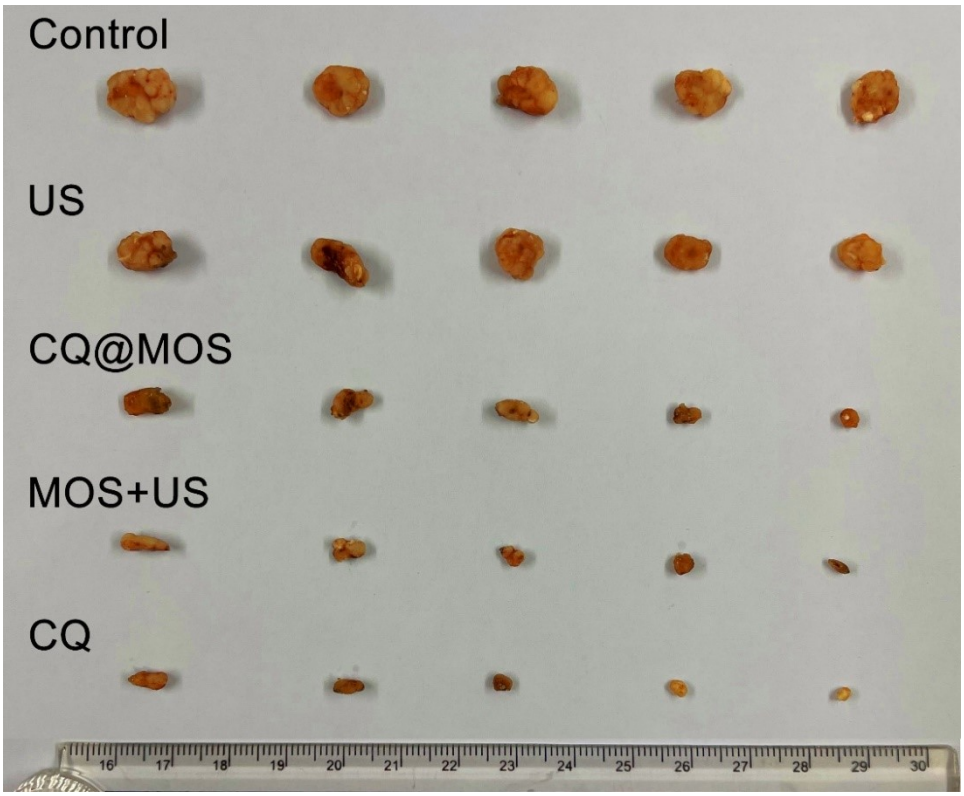

Figure S9| Image of tumors harvested from mice after the completion of various treatments (saline, US, CQ@MOS, MOS+US and CQ).

Due to the enhanced sono-cavitation effect of MOS, the MOS+US treatment

introduced massive reactive oxygen species and powerful mechanical waves into tumor cells, leading to significant anti-tumor effects. In addition, due to the incomplete release of CQ from CQ@MOS, CQ@MOS showed a slightly lower tumor suppression effect compared with CQ. Therefore, US irradiation was applied to trigger the rapid release of CQ from MOS. The tumor inhibition efficiency of CQ@MOS, MOS+US, CQ and CQ@MOS are 71.6%, 83.0%, 86.3% and 97.5%, respectively.

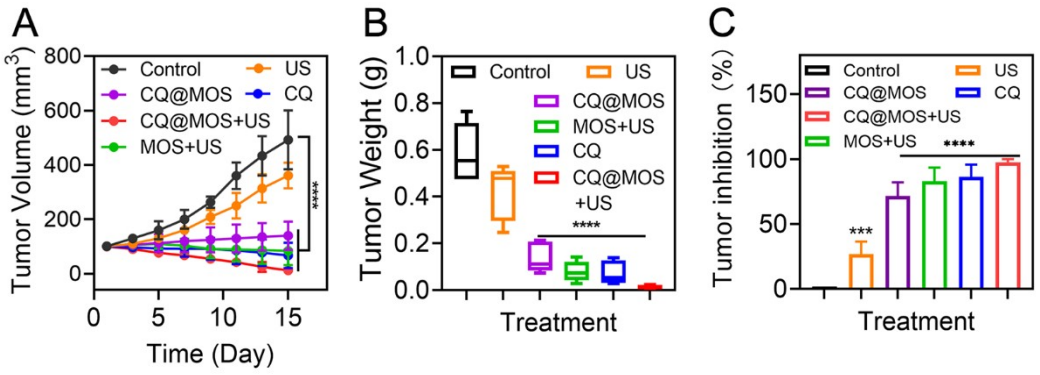

Figure S10| (A) Growth curves of tumors for mice treated with saline, US, CQ@MOS, MOS+US, CQ and CQ@MOS+US (n=5 mice per group). (B) Average tumor weight of mice subjected to the specified treatments for 15 days. (C) Tumor inhibition efficiency of various formulations after 15 days treatment. These data in (A), (B) and (C) are expressed as the mean ± SD of five independent samples. ***p < 0.001, ****p < 0.0001, vs. the control group.

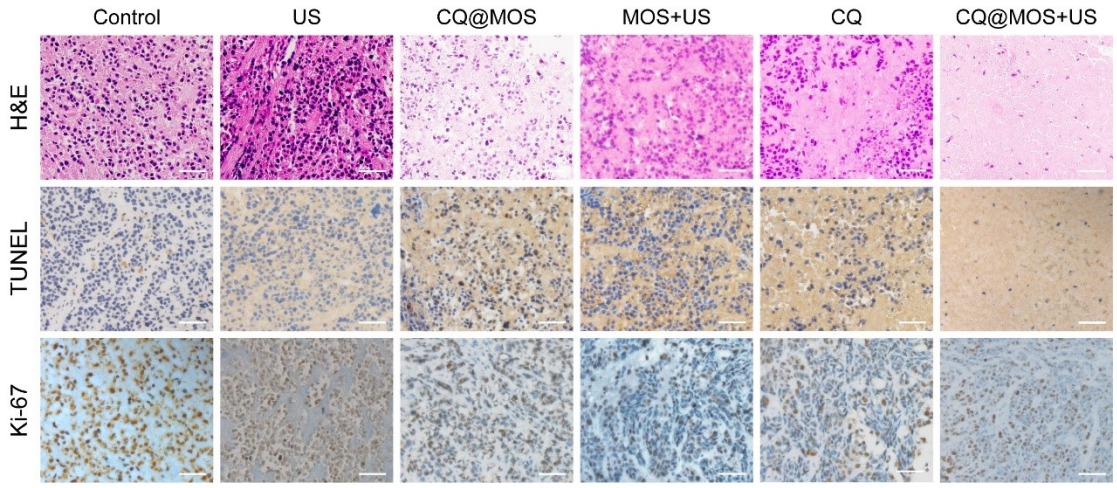

Figure S11| Histological photographs of H&E, TUNEL (DNA fragmentation) and Ki-67 (cell proliferation) stained tumor sections in diverse groups. Scale bar: 50 μm.

The treatments with CQ@MOS, MOS+US, CQ, and CQ@MOS+US induced significant 4T1 tumor cell death and proliferation inhibition, as evidenced by a notable reduction in purple nuclei and brown Ki-67 signals in 4T1 tumor tissues. Moreover, these treatments led to remarkable apoptosis of 4T1 tumor cells, as evidenced by high

brown TUNEL signals.

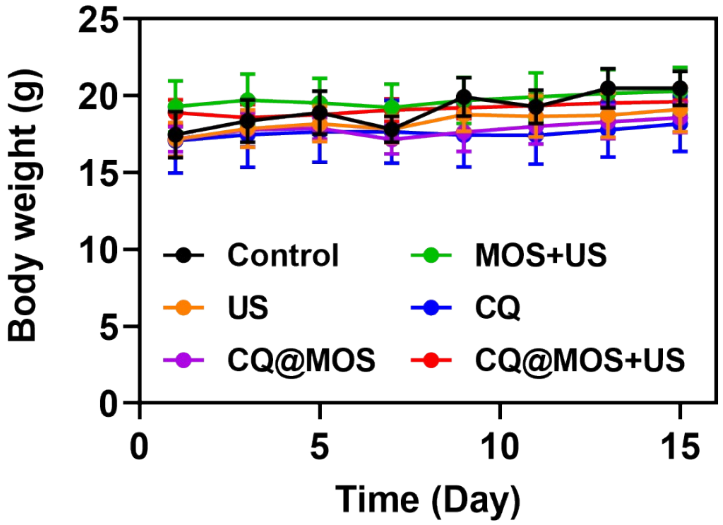

Figure S12| Body weight of 4T1 tumor-bearing nude mice over the 15-day treatment period in different groups via intra-tumoral injection (n=5 biologically independent samples).

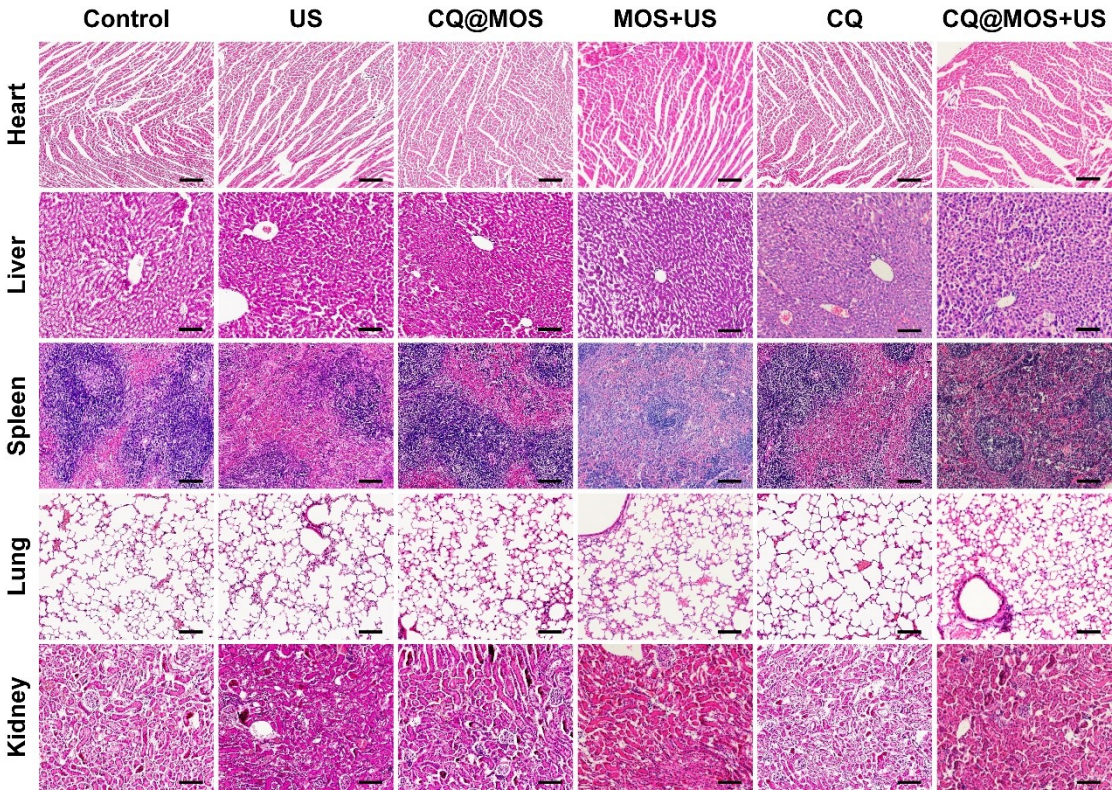

Figure S13| H&E staining images of primary organs from 4T1 tumor-bearing nude mice following various treatments via intra-tumoral injection. Scale bar: 100 μm.

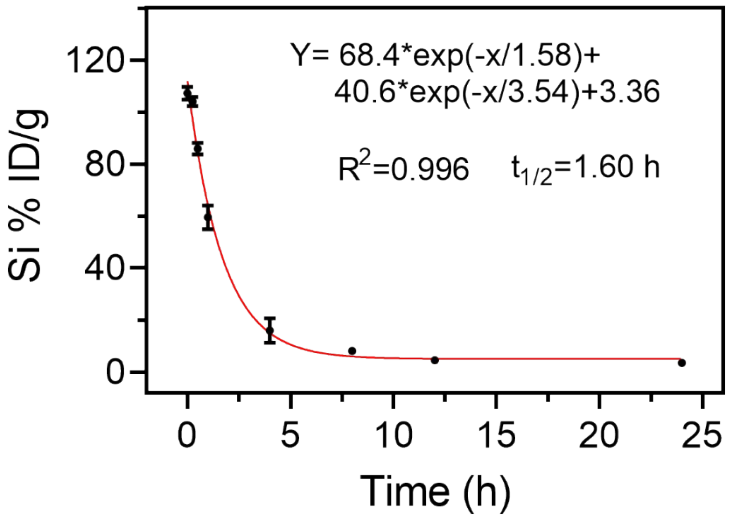

Figure S14| Blood circulation curve of Si content after intravenous administration of CQ@MOS.

The time-dependent blood circulation curves showed that the blood half-life of CQ@MOS was 1.60 h. Data are presented as mean ± SD (n = 3).

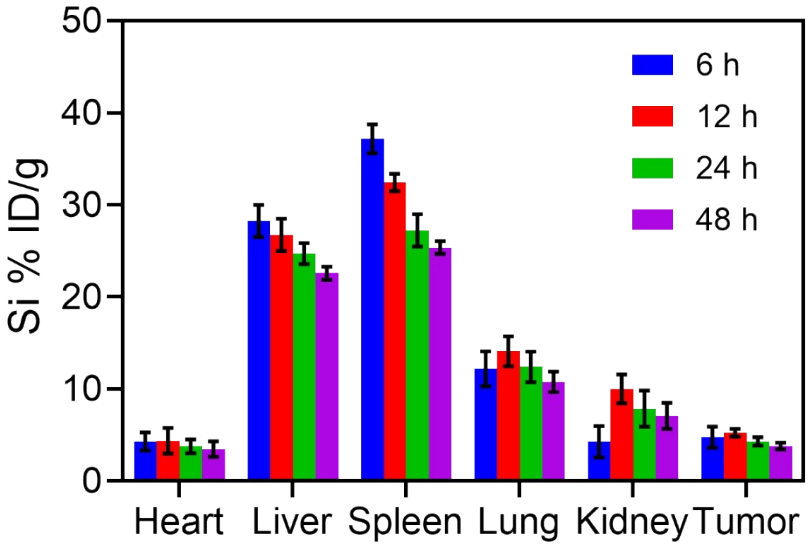

Figure S15| Biodistribution of Si in main organs and tumor after intravenous injection with CQ@MOS for 6, 12, 24 and 48 h.

The biodistribution results indicated that CQ@MOS could be effectively accumulated at tumor sites because of the enhanced permeability and retention (EPR) effect and relatively small diameter (about 205 nm) of CQ@MOS.

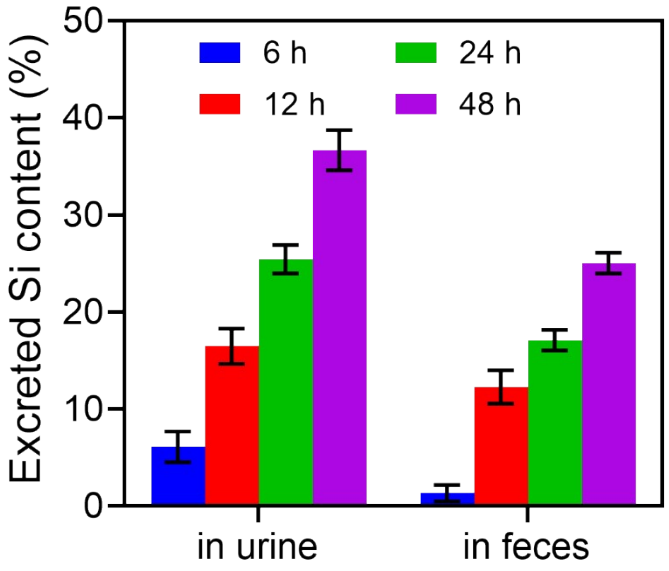

Figure S16| Accumulated Si contents in urine and feces of female ICR mice after intravenous administration of CQ@MOS for 6, 12, 24 and 48 h.

After 48 h of administration, a significant amount of Si component was found in the feces and urine of the mice, indicating that CQ@MOS could be effectively eliminated through both the fecal and renal systems.

3. Supplementary tables

Table of contents

Gene	Primer F	Primer R
GADPH	GAGTCGGTGTGAACGGATTTG	TGTAGACCAGTTAGTTGAGGTCA
Bax	TAATGCCCGTTCATCTCAGTCC	TGGGCGTCCCAAAGTAGGA
Apaf-1	GGTAATTTAGCACATGAACATCCAA	ACTCTAACAGCAGAGGTCACA
caspase-9	CCTGCCCGCTGTTTGGA	AGGCTGGTAAATGCCACACA
caspase-3	CAGGGCCGAAAAGGAATTGG	GACTGTGAGATACTCGCCCTG
c-Jun	CCGAGAGCGGTGCCTACGGCTACAG	GACCGGCTGTGCCGCGGAGGTGAC
Fas-L	TCATCTTGGGCTCCTCCAGGGTCAG	GGCTTTGGTTGGTGAACTCACGGAG
TNF-α	GCGACGTGGAACTGGCAGAAG	GGTACAACCCATCGGCTGGCA
Bid	AATGGCCTTCATATCATCCACACA	GGGAACCTGCACAGTGGAAATAA
JNK	AACTGTTCCCCGATGTGCT	ACAAATCTCTTGCCTGACTGG
ASK1	GCCTTCCCTGTTTTATCATCTCG	CACTGTGTTCTTCTGGCAAATGAT

Table S1| Primer sequences are reported 5'-3'.